Correlation of disease evolution with progressive inflammatory cell activation and migration in the IL-4 transgenic mouse model of atopic dermatitis

Lin Chen,* O. Martinez,†
P. Venkataramani,* S.-X. Lin,*
B. S. Prabhakar† and L. S. Chan*†‡

*Departments of *Dermatology & †Microbiology/
Immunology, University of Illinois at Chicago,
College of Medicine and ‡Medicine Service, VA
Jesse Brown Medical Center, Chicago, USA*

Summary

Atopic dermatitis is a chronic inflammatory skin disease characterized by inflammatory cell infiltration in the skin. In order to assess the roles of inflammatory cells in this disease, we analysed the activation status and surface markers of various leucocytes in the IL-4 transgenic mouse model of atopic dermatitis, by flow cytometry, immuofluorescence microscopy, and T cell proliferation assays. The studies were performed with a nontransgenic mouse control and transgenic mice at three disease stages: before disease onset, early skin disease, and late skin disease, so that we can delineate the immunological sequence of events. As the skin disease evolves, the skin draining lymph node cells from IL-4-Tg mice show a spontaneous proliferation and a progressively enhanced proliferative response to stimulants including anti-CD3, Con A, PHA, and Staphylococcus enterotoxins A and B. As the disease evolves, the percent of lymphoid organ T cells expressing activation molecules (CD44 and CD69) and costimulatory molecules (ICOS and PD-1) are progressively increased; the percent and total number of T cells are reduced in an incremental manner in the secondary lymphoid organs while the number of T cells infiltrating the skin increases in an incremental fashion; the total number of dendritic antigen presenting cells, macrophages, and NK cells gradually increases in the lymphoid organs. Collectively, our results suggest that there is a continued and progressive migration of activated inflammatory cells from the secondary lymphoid organs into the skin where they participate in immune responses resulting in the pathology associated with inflammation.

Keywords: atopic dermatitis, animal model, T cells, antigen-presenting cells, proliferation

Introduction

Atopic dermatitis (AD) is a common, chronic, pruritic, inflammatory skin disease with a life time prevalence of 10–20% in children [1,2]. The prevalence of AD has steadily increased in the developed nations during the past few decades [2]. Extensive studies have been conducted in an attempt to understand the pathogenic mechanism of this disease in humans. The general consensus is that AD is an immune-mediated skin disease characterized by a predominance of Th2 type cytokines in early skin lesions followed by the presence of both Th1 and Th2 type cytokines in late skin lesions [3,4]. Several groups reported that in the dermis of

human AD, there are T cell infiltrates including CD4+ and CD8 cells+, with CD4+ cells predominating over CD8+ cells [5–8]. Another study has shown that AD fails to occur in the absence of αβ TCR+ T cells in a mouse model of AD induced by epicutaneous application of allergen, further supporting the role of T cells in AD pathogenesis [9]. Additionally, other inflammatory cells, mast cells, eosinophils, and macrophages have been identified in the skin lesions of human AD [10]. Although outstanding progress has been made in the investigation of AD in human patients, there are many limitations that prevent complete understanding of AD. The first one is that due to ethical reasons one cannot perform sequential analysis of immune response in the skin during the

pathogenesis of the disease. Another limitation is the inability to perform studies that require invasive procedures on vital organs due to obvious safety and ethical concerns. Here we take advantage of the availability of an animal model of IL-4-Tg mice [11] that spontaneously develop a chronic, pruritic, inflammatory skin disease that closely resembles human AD based on clinical, histological, bacteriological, and serological characteristics and fulfills the clinical diagnostic criteria for human AD [11,12]. We performed systematic studies on the controlled and affected skin and secondary lymphoid organs of non-Tg mice, Tg mice before skin disease onset (Tg-BO), Tg mice with early skin disease (Tg-EL) and Tg mice with late skin disease (Tg-LL) in order to gain insights into the evolution of immune response at different disease stages. By correlating the activating status and numerical changes of the inflammatory cells with the disease progression, we may delineate pathomechanisms responsible for the disease induction and progression.

Because previous studies using human subjects are limited in scope. we carried out, in this study, a detailed phenotypic analysis of the inflammatory cells in the secondary lymphoid organs, spleen and skin draining lymph nodes (LNs), and in the skin by examining their relative composition and absolute cell number, their surface activation molecules, and their costimulatory molecules. Spontaneous as well as mitogen or superantigen induced T cell proliferation was also investigated. Our results showed that:

- As the disease progresses, the T cells from IL-4-Tg mice showed a progressively enhanced proliferative response to stimulants, correlating with the disease progression;
- As the disease progresses, the percent of T cells expressing certain activation molecules and costimulatory molecules were progressively increased;
- As the disease progresses, the percent of T cells among all leucocytes and the absolute T cell numbers were reduced in an incremental manner in the secondary lymphoid organs, while the number of T cells infiltrating the skin increased in an incremental fashion;
- As the disease progresses, the absolute number of antigen presenting cells, macrophages, and NK cells showed gradual increases in the lymphoid organs. Collectively, our results suggest that there is a continued and progressive migration of activated inflammatory cells from the secondary lymphoid organs into the skin that might result in the pathology associated with AD.

Materials and methods

Mice

Four to 12 week old IL-4-Tg mice were used in the experiments [11]. This mouse model was achieved by epidermal transgenic expression of IL-4 using a construct containing the basal keratinocyte keratin-14 (K14) promoter/enhancer, rabbit beta-globin intron, murine IL-4 cDNA, and the K14 polyA tail. IL-4-Tg mice develop inflammatory skin disease resembling human AD [11]. After a period of a few years of the establishment of this model, all IL-4-Tg mice began to develop skin lesions within 4–8 weeks after their birth. The non-Tg offspring served as age-matched, littermate controls. The average ages for non-Tg, Tg-BO, Tg-EL or Tg-LL are 8, 5, 6 and 8 weeks, respectively. All mice were housed in the special pathogen-free room and fed with standard water and mouse chow.

Genotyping

Mice born from heterozygous IL-4-Tg mouse parents were genotyped for confirmation of their positive Tg status. The method we used is the following: A small quantity of tail (about 0·5 cm long) was clipped from each mouse to extract DNA. The skin of the clipped tail was removed by scrapping and the remaining tissue was digested in the presence of protease K (100 µg/ml) in an enzyme buffer consisting 10 mM Tris (pH 8·0), 100 mM NaCl, and 1 mM EDTA, at 55°C overnight. After centrifugation for 5 min at 12 000 *g*, the supernatant was collected and boiled at 100°C for 20 min, the resulting solution (5 µl per 25 µl reaction volume) was used for genotyping by standard PCR method [11] using mouse IL-4 sequence-specific primer pair. The PCR was performed in a Perkin-Elmer GeneAmp 2700 Thermocycler (Applied Biosystems, Foster City, CA, USA) using the following cycling parameter: 94°C, 1 min; 55°C, 1 min; 72°C, 1 min after preheating at 94°C for 4 min for 35 cycles, followed by a single 10 min extension at 72°C. A 357 bp DNA band corresponding to the mouse IL-4 nucleotide 70–427 [13] was visualized in a 1·5% agarose gel stained with ethidium bromide.

Disease phenotype classification

This section was described in a previous publication [14]. In brief, Tg-EL (early or acute lesion) defines skin lesions developed for no more than one week in duration. Tg-LL (late or chronic lesion) defines skin lesions developed for more than 3 weeks in duration. Tg mice before onset of any noticeable skin lesion is classified as Tg-BO. Clinically, the late lesions were more severe and had more scaling than the early lesions; histologically, EL skin was characterized by moderate increase of epidermal thickness (acanthosis), dermal and epidermal leucocyte infiltration, and spongiosis, resembling that of an acute inflammation in human AD [15]. LL skin was distinguished from EL samples by substantial increase of acanthosis, leucocyte infiltrate, and the presence of parakeratosis, a histological marker for chronic inflammation in human AD [15]. Serologically, IgG1 and IgG2a (not IgE) in Tg-LL mice were significant higher than that in Tg-EL mice (unpublished observation).

Antibodies and reagents

Monoclonal antibodies (mAbs) were used for FACS analysis. FITC or PE hamster anti-mouse CD3 and PE hamster anti-mouse CTLA-4 were obtained from BD Bioscience (San Diego, CA, USA). FITC rat Abs to mouse IA-IE (MHC II), Mac-3, DX5; FITC hamster anti-CD11c, PE hamster Abs to mouse inducible costimulatory molecule (ICOS), CD28, programmed death 1 (PD-1), CD69 and CD80; PE rat Abs to mouse CD86, B7 homolog (B7 h, B7RP-1, ICOSL), PD–1 ligand 2 (PD-L2, B7-DC), and CD44 were obtained from eBioscience (San Diego, CA, USA). Rat anti-mouse CD16/32 (eBioscience) was used to block Fc receptors. Isotype controls used for flow cytometry were FITC or PE rat IgG2a and IgG2b, FITC rat IgG1 and IgM, and PE hamster IgG (eBioscience). For skin *in situ* immunofluorescence microscopy, primary mAbs used include rat Abs to mouse CD11a, IA-IE, CD23 (FceRII) from BD Bioscience, San Diego, CA, and rat Abs to mouse CD3, CD4 and CD8 from Southern Biotech, Birmingham, AL, USA. The secondary Abs used were Alexa Fluor 488-conjugated goat anti-rat IgG and goat anti-rat IgM (Molecular Probes, Eugene, OR, USA). Isotype controls used for skin immunofluorescence include rat IgG1, IgG2a, and IgG2b (BD Bioscience).

Immunofluorescence microscopy

Lesional and normal tissues (about 1 cm^2) were taken from the ears of IL-4-Tg mice at EL or LL stage and non-Tg mice, respectively. Since all ear tissues were affected, nonlesional skin of diseased Tg mice (Tg-NL) tissues were taken from the back of IL-4-Tg with disease which is distant from any lesion. The tissue samples were first placed in 0·2% paraformaldehyde/PBS for overnight and then in a 30% sucrose/PBS solution for overnight at 4°C. Thereafter, the samples were embedded in Tissue-Tek® OCT (Sakura Finetechnical, Tokyo, Japan) at −20°C and cut with a Leica CM1850 cryostat (Leica Microsystems, Nussloch, Germany). For immunofluorescence staining, the 8 µm cryo-sections were incubated with various primary Abs followed by Alexa Fluor 488-conjugated secondary Abs diluted in 1% BSA/PBS. After staining, the sections on each slide were mounted using glycerol/PBS at a 1 : 1 ratio, and examined under an Olympus BX60 fluorescence microscope with a high power objective lens (40×). Five different areas for each tissue sample were counted to determine the number of stained cells. The average number of positively stained cells was then calculated as cells per high powered field (HPF). Fifteen samples from each group (non-Tg, Tg-NL, Tg-EL, and Tg-LL) were included in this study. All Abs were titrated in preliminary experiments to determine an optimal dilution.

Fluorescence activated cell sorting (FACS) analyses

Skin draining LNs and spleens were collected from Non-Tg, IL-4-Tg-BO, Tg-EL, and Tg-LL mice. Mononuclear cells in the spleens were enriched by gradient density centrifugation using Lympholyte-M (Cedarlane, Ontario, Canada). A total of 1×10^6 lymph node cells or mononuclear cells from the spleen were first incubated with anti-mouse CD16/32 in cold PBS/2% FCS/0·1% NaN$_3$ for 10 min on ice to block Fc receptors. Cells were then labelled with FITC or PE-conjugated monoclonal Abs against selected cell surface antigens as stated in the Antibodies and Reagents section above. Live cells were gated based on 7-aminoactinomycin D (BD Bioscience) uptake. FACS analyses were performed on the Calibur FACS system (BD Bioscience). In all experiments, samples with FITC or PE-conjugated isotype controls were also analysed. All Abs were used at a final concentration of 5 µg/ml. LNs and spleen cells from three to six mice were pooled for each assay. For FACS analyses of skin samples, ear biopsies obtained from early and late skin lesions were first washed in 70% ethanol, and then cut into small pieces in trypsin-GNK solution containing 200 µg/ml DNase and stirred for 20 min at 37°C [16]. The single cell suspension was filtered through a cell strainer and washed with RPMI 1640 medium, and then was labelled with PE- or FITC-conjugated monoclonal Abs to mouse CD11a, CD3, CD4, CD8 or IA-IE and analysed as described above.

Determining absolute numbers of leucocytes

Cells from spleen and skin draining lymph nodes from Non-Tg, or from IL-4-Tg mice were suspended in RPMI 1640 medium. Single cell suspensions were then counted using a haemocytometer. The total number of the cells was then multiplied by the percentage of CD3, CD11c, Mac3 and DX5/CD11a determined by the FACS analysis to calculate the absolute numbers of each cell population in the secondary lymphoid organs.

Skin draining LN cell proliferation assay

Skin draining LNs were obtained from non-Tg and IL-4-Tg mice at different stages of AD. A total of 1×10^5 cells in single cell suspension were obtained and cultured in RPMI 1640 medium with 10% FCS either with or without anti-CD3e (1 µg/ml) (eBioscience), Concanavalin A (Con A, 5 µg/ml), Phytohemagglutinin (PHA, 5 µg/ml), *Staphylococcus* enterotoxin B (SEB, 25 ng/ml) (Sigma, St. Louis, MO, USA), *Staphylococcus* enterotoxin A (SEA, 25 ng/ml) (Toxin Tech, Sarasota, FL, USA) in a total volume of 200 µl for 72 h in 37°C and 5% CO$_2$ environment. A preliminary study determined the optimal concentrations of mitogens or superantigens. The cell proliferation assay in triplicate was performed using a Cell Counting Kit-8 (CCK-8) purchased from Dojido (Kumamoto, Japan). Briefly, after 72 hrs' culture 20 µl of WST-8 was added to each well and incubated for an additional 4 h at 37°C. WST-8 is a water-soluble tetrazolium salt, which is reduced by dehydrogenase activities of viable cells to produce a yellow colour formazan dye. The

total dehydrogenase activity of viable cells in the medium, determined by the intensity of the yellow colour measurable by spectrometry, can then be used to determine the relative amounts of viable cells. The absorbance at 450 nm was read in a μQuant microplate reader (Bio-TEK, Inc., Winooski, Vermont) with a reference wavelength at 600 nm. Data are expressed as mean ± SD in triplicate.

Statistical analysis

All experimental data were expressed as mean ± SD. The significance of the variation among different groups was determined by One-Way ANOVA Analysis and the difference between two groups was determined by Tukey-Kramer Multiple Comparison Test using GraphPad Instat Software. *P*-value <0·05 was considered significantly different.

Results

Percent of T cells decreases while that of activation marker-expressing T Cells increases in the secondary lymphoid organs of diseased mice

We used FACS to determine the percent of different subsets of leucocytes in secondary lymphoid organs in Tg mice before disease onset and during different stages of the disease, relative to non-Tg mice. First, to our surprise, the percent of T cells in both LNs and the spleen decreased remarkably in IL-4-Tg mice (Fig. 1a). The percent of CD3+ T cells among CD11a+ leucocytes in LNs were 76·61% in non-Tg mice, 67·70% in Tg-BO mice, and was down to 59·25% in Tg-EL mice, that was further reduced to 26·87% in Tg-LL mice (Fig. 1a). This reduction is even more dramatic in the spleen, where the percent CD3+ T cells among CD11a+ leucocytes were 56·57% in non-Tg mice, down to 32·35% in Tg-BO mice, 28·27% in Tg-EL mice, and to only 1·91% in Tg-LL mice (Fig. 1a). The absolute numbers of CD3+ cells in the spleen gradually decreased as the same pattern of percentage changes showed above, while the numbers in LNs remained relatively constant at Tg-BO and Tg-EL stages and increased dramatically at the Tg-LL stage (Fig. 1b). However, there was no significant change of the frequencies of two major subsets, CD4+ and CD8+ cells, among all T cells, at different stages of the disease, with the exception of noticeable reduction of CD4+ cells in the Tg-LL stage (Fig. 1c,d). If the data obtained from LNs and spleens were calculated together, both the average percent of T cells and the total combined number of T cells were was progressively reduced (Fig. 1a,b). These results in our mouse AD model were similar to the findings in the peripheral blood of patients with severe or mild AD, which showed that T cells are significantly decreased compared to the levels in healthy blood donors [17].

Next, we determined the activation status of T cells in these secondary lymphoid organs, using FACS analysis. We found that the percentage of T cells expressing two activation markers, CD44 and CD69, increased in both major T cell subsets in the Tg-BO mice, Tg-EL mice, and Tg-LL mice, relative to non-Tg mice (Fig. 1e–h). We also examined the expression of costimulatory molecules on the T cells in these secondary lymphoid organs. We found that while the percentage of CD4+ and CD8+ cells expressing CD28 were slightly reduced as the disease progressed in the Tg mice, in comparison to non-Tg mice (Fig. 1i,j), the percentages of two other costimulatory molecules, ICOS- and PD-1, expressed on CD4+ and CD8+ cells, generally increased as the disease progressed (Fig. 1k–n), paralleling the increase of the activation markers of CD44 and CD69 on the same subsets (Fig. 1e–h). We were unable to detect the presence of CTLA-4 surface markers on these T cell subsets.

Lymphoid organ dendritic cells decrease in the percentage and increase in total number as the disease progresses

Recognizing the general importance of dendritic cells (CD11c+) in the adaptive immune response [18], we also investigated their presence and their characteristics in our model by FACS in spleen and LNs. While the average percent of CD11c+ cells among CD11a+ leucocytes in the spleens and LNs slightly decreased in the diseased mice (Fig. 2a), the total combined numbers of CD11c+ cells had an increasing trend, when compared to that of non-Tg mice (Fig. 2b). The average percentages of the four costimulatory molecules that we examined (CD80, CD86, B7 h, and B7-DC) showed no significant changes, either slightly increased or slightly decreased, in the diseased mice, comparing to that of non-Tg mice (Fig. 2c–f). Interestingly, the highest percent and the total number of CD11c+ dendritic cells, as well as the highest percent of CD86+, B7 h+, and B7-DC+ dendritic cells were observed in the Tg-BO mice (Fig. 2).

Monocytes/macrophages increase in secondary lymphoid organs as the disease progresses

We next investigated the presence of monocytes and macrophages by FACS analyses because of their special role as antigen-presenting cells (APCs). We found that both the percentages and absolute numbers of Mac3+ cells of CD11a+ leucocytes increased in the spleen and LNs, as the disease progresses (Fig. 3). The combined calculations of the data for both LNs and spleens showed identical trends (Fig. 3).

NK cells increase in the secondary lymphoid organs as the disease progresses

We also investigated the frequency change of NK cells using Ab against DX5 marker. We found that although they repre-
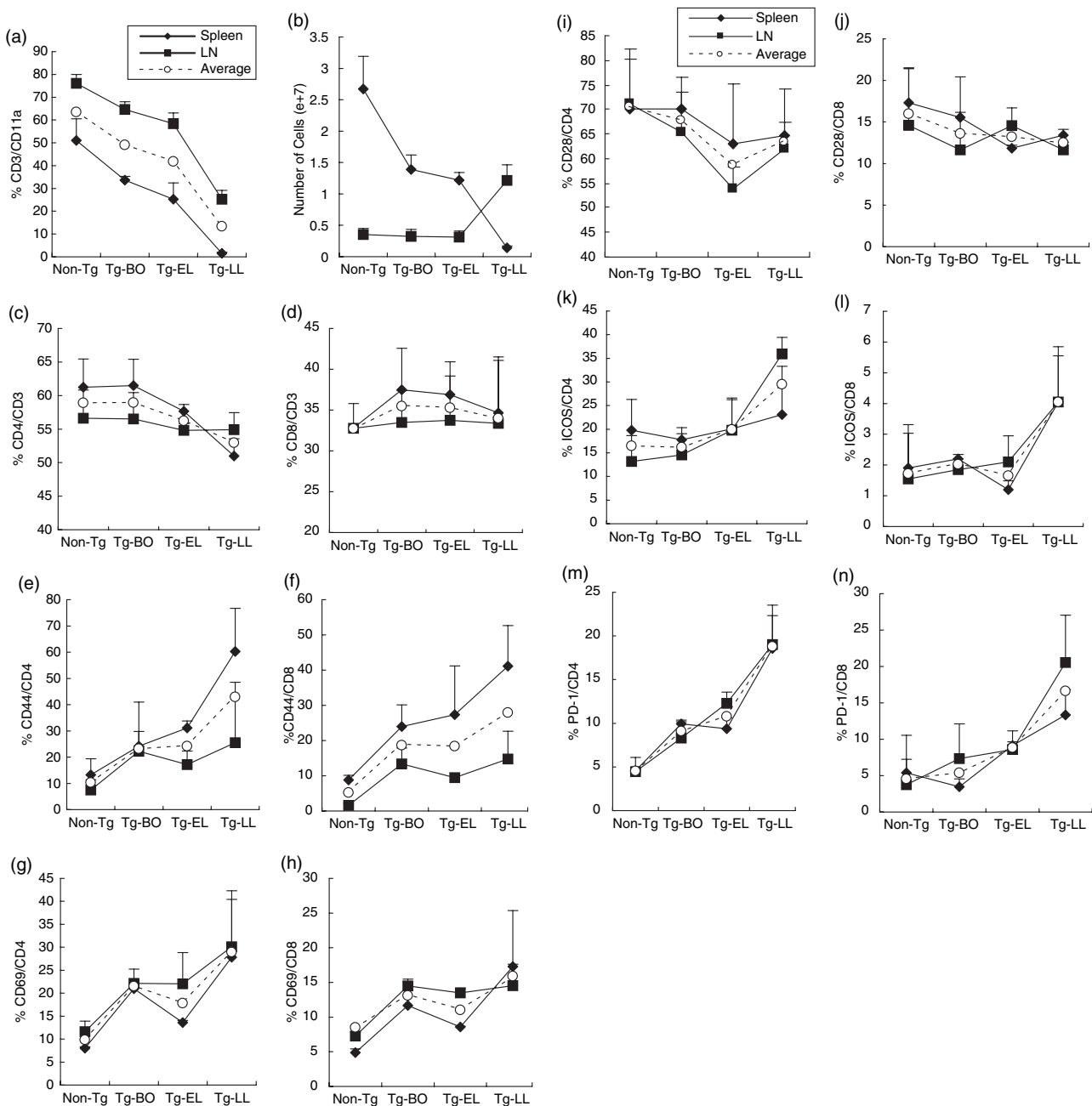
Fig. 1. As the disease progresses T cells in the secondary lymphoid organs decrease progressively while exhibiting increased expression of activation molecules and costimulatory molecules ICOS and PD-1. Spleen and LN cells were collected from Non-Tg and Tg mice at different stages of disease, and then stained with specific Abs for the given cell surface molecules, followed by FACS analyses. (a) percentage and (b) absolute number changes of CD3+ cells; (c) and (d), the percentage of CD4+ and CD8+ cells in CD3+ cells; (e) and (f) (g) and (h) represent percentage of CD44+ and CD69+ cells in CD4+ and CD8+ cells. (i) and (j), (k) and (l), (m) and (n), represent, respectively, percentage of CD28+, ICOS+ and PD-1+ cells in CD4+ and CD8+ cells. Data were the average of three experiments. ◆ Spleen, ■ LN, ○ Average percentage of spleen and LN (a, c–h, i–n).

sent a small subset of CD11a+ leucocytes, they showed some increase in both frequency and absolute numbers in the spleen and LN as the disease progresses (Fig. 4). Identical increasing trend was visualized in the combined calculations of the data from both LNs and spleens (Fig. 4).

Skin draining LN cells exhibit progressively enhanced proliferative states as the disease progresses

To examine the activation state of cells in the secondary lymphoid organ, especially T cells, skin draining LN cells from
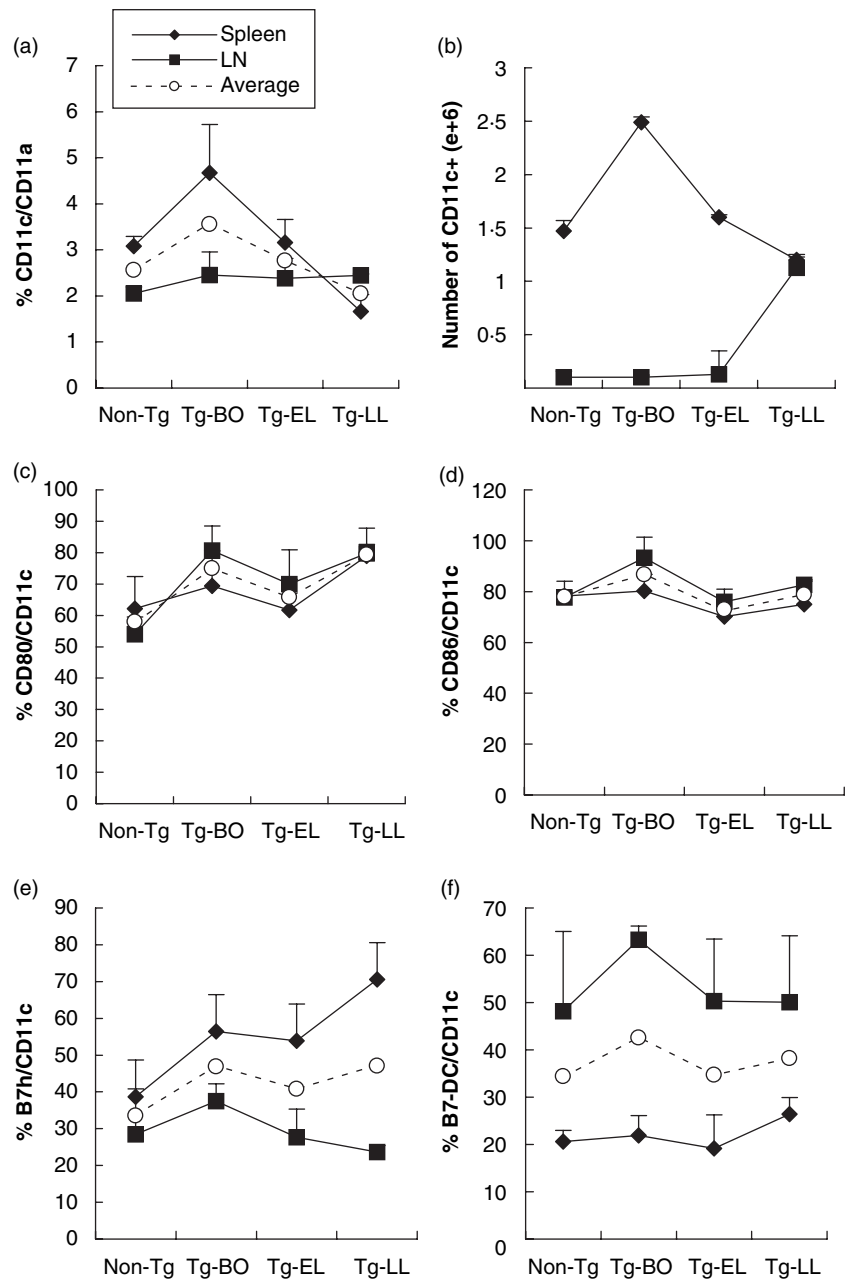
Fig. 2. The highest percent and total number of CD11c+ dendritic cells, as well as the highest percent of costimulatory molecules barring dendritic cells, occurred in the Tg mice before onset. Spleen and LN cells were collected from Non-Tg and Tg mice at different stages of disease, and then stained with specific Abs against CD11a, CD11c, CD80, CD86, B7 h and B7-DC, followed by FACS analyses. (a) percentage and (b) absolute number changes of CD11c+ cells; (c-f) represent percentages of CD80+, CD86+, B7 h+ and B7-DC+ cells, respectively, in CD11c+ cells. Data were obtained from the average of three experiments. ◆ Spleen, ■ LN, ○ Average percent of spleen and LN (a, c–f).

different stages of disease were examined for their ability to spontaneously proliferate in the absence of external stimulus. Cells obtained from skin draining LNs were used instead of that from spleen because of near total depletion of T cells in the spleens of mice with late skin lesions (Fig. 1a,b). As shown in Fig. 5, Cells from Tg mice at all stages of the disease proliferated spontaneously and in a progressively enhanced manner. Cell proliferation from Tg mice with either early or late lesions was significantly higher than that of non-Tg mice ($P < 0.01$ and <0.001, respectively). In addition, the cell proliferation in Tg mice with late lesions was significantly higher than that noted in cells from Tg mice either before onset ($P < 0.001$) or with early disease

($P < 0.001$). The cell proliferation in Tg-BO mice (0.370 ± 0.003) is also higher than that of non-Tg mice (0.242 ± 0.001), although no statistically significant difference was observed ($P > 0.05$) (Fig. 5). To examine the activation states of the cells in the secondary lymphoid organ in response to stimulants, LN cells from different stages of disease were examined for their proliferation in the presence of various stimulants (anti-CD3, Con A, and PHA) or superantigens (SEA and SEB). Anti-CD3 induced the strongest cell response, and SEA induced a slightly stronger response than SEB among the two superantigens tested (Fig. 5). Regardless of the type of stimulant, cells from Tg-LL mice showed the highest response, followed by cells from Tg-EL

Fig. 3. The increases of Mac+ cell frequency and number in the secondary lymphoid organs occurred predominantly at the Tg-LL mice. Spleen and LN cells were collected from Non-Tg and Tg mice at different stages of disease, and then stained with specific Abs against CD11a and Mac3, followed by FACS analyses. (a) percentage and (b) absolute number changes of CD11a+/ Mac3+ cells. Data were obtained from the average of three experiments ◆ Spleen, ■ LN, ○ Average percent of spleen and LN (a).
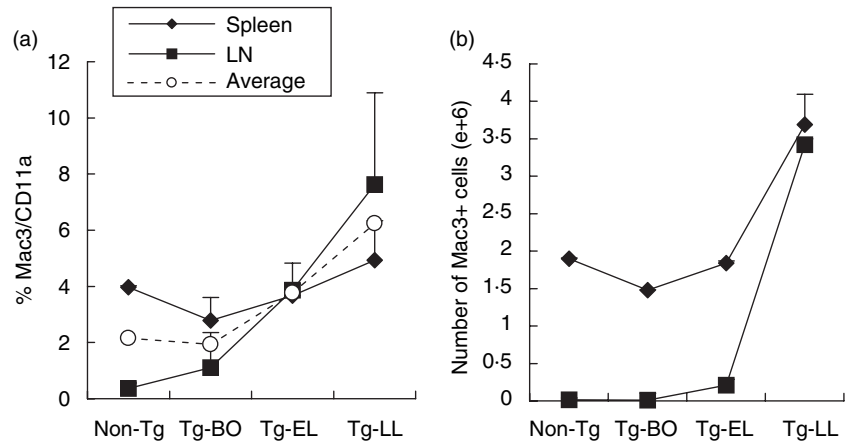

Fig. 4. As the disease progresses, the frequency and absolute numbers of DX5+ cells in the lymphoid organs showed an increasing trend. Spleen and LN cells were collected from Non-Tg and Tg mice at different stages of disease, and then stained with specific Abs against CD11a and DX5, followed by FACS analyses. (a) percentage and (b) absolute number changes of DX5+ cells. Data were obtained from the average of three experiments ◆ Spleen, ■ LN, ○ Average percent of spleen and LN (a).
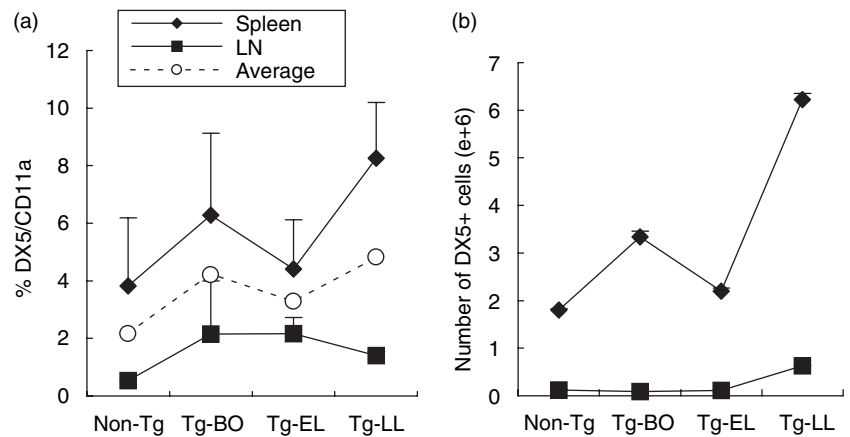
mice, Tg-BO mice, and from non-Tg mice (Fig. 5). Cells from diseased mice (Tg-EL and Tg-LL mice) showed significantly higher response than the cells from non-Tg mice, in response to all stimulants, except Con A ($P < 0.01$ to $P < 0.001$). Furthermore, cells from Tg-LL mice showed significantly higher responses than the cells from Tg-BO mice, to all five stimulants ($P < 0.05$ to $P < 0.001$). In addition, the cells from Tg-EL mice showed significantly higher prolifer-
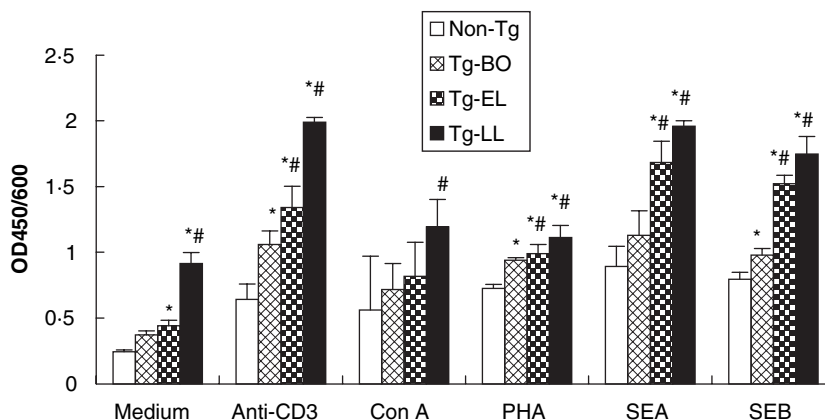
Fig. 5. As the disease progresses, skin draining LN cell spontaneously proliferated in the absence of stimulant and proliferated in a progressively enhanced manner in response to mitogens and superantigens. LNs were obtained from one mouse of each group including non-Tg Tg-BO, Tg-EL and Tg-LL. A total of 1×10^5 cells in single cell suspension were obtained and cultured with or without anti-CD3 (1 μg/ml), Con A (5 μg/ml), PHA (5 μg/ml), SEA (25 ng/ml) or SEB (25 ng/ml) for 72 h, and then WST-8 was added for an additional 4 h. The absorbance at 450 nm was read in a microplate reader with a reference wavelength at 600 nm. Data are expressed as mean ± SD in triplicate. *Statistical significance *versus* Non-Tg mice; #Statistical significance *versus* Tg-BO. Similar results were obtained in two additional experiments.

(a)
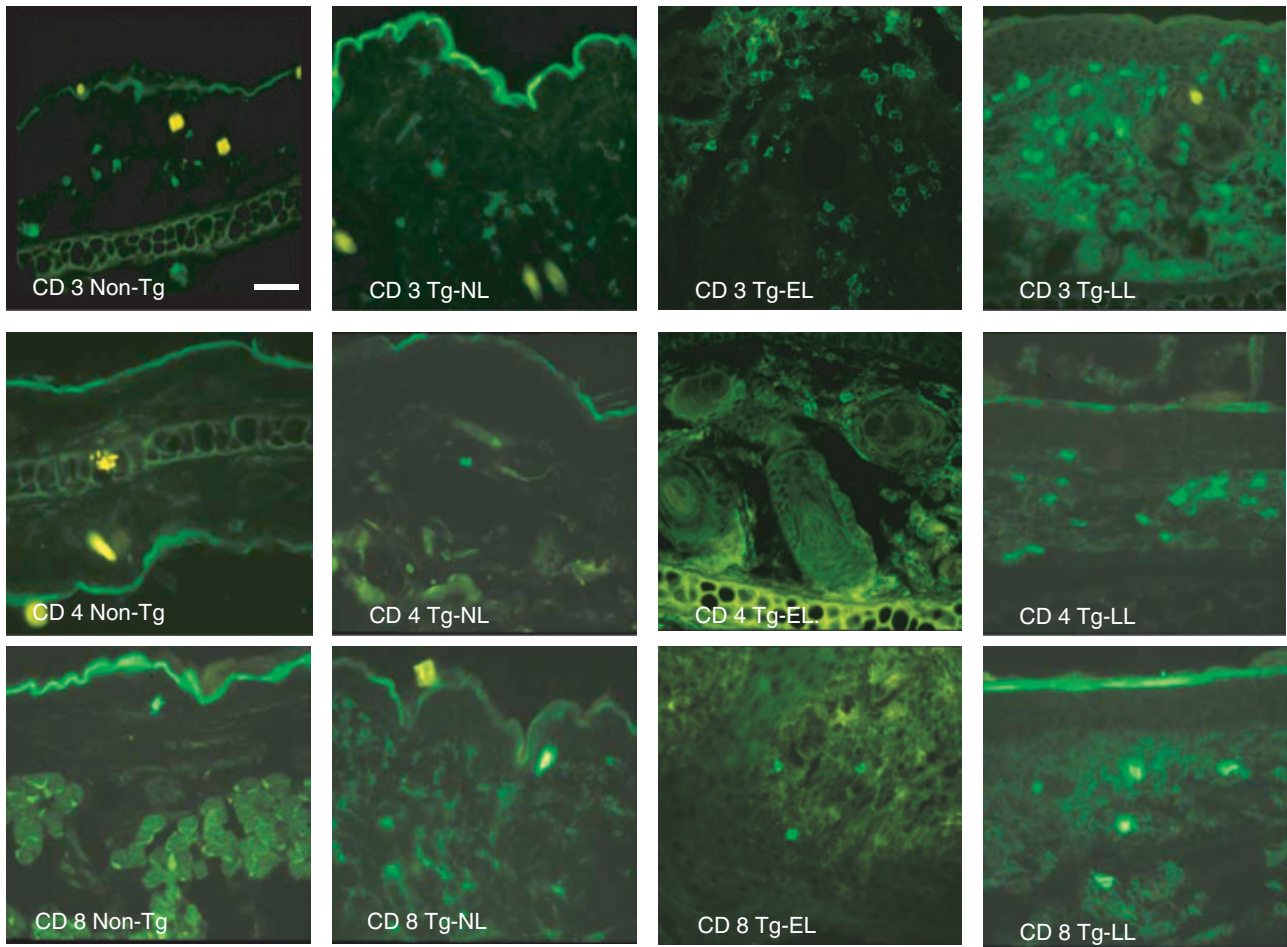
Fig. 6. As the disease progresses, inflammatory cells infiltrate progressively in diseased skin. (a) Immunofluorescence microsopic examination. Frozen sections were incubated with primary rat monoclonal Abs against CD3 (upper row), CD4 (middle row), CD8 (lower row), and MHC II (IA-IE) (not shown), followed by Alexa fluor 488-conjugated goat anti-rat IgG Abs. The sections were then examined under a fluorescence microscope. Illustrations shown are representatives of 15 samples examined. NL, nonlesional skin from diseased mice. Scale bar = 38 µm. (b–e) Bar graph presentations of the inflammatory cell number in the skin. The sections on each slide were examined and five different areas in each sample ($n = 15$) were counted to determine the average number of a particular cell present per HPF (at 40× objective lens). *Statistical significance *versus* Non-Tg mice; #Statistical significance *versus* Tg-NL. (f) FACS analyses of CD3+, CD4+, CD8+ and MHC II cells in the skin lesions. The single cell suspension from early and late lesional ears was labelled with PE- or FITC-conjugated monoclonal Abs to mouse CD11a, CD3, CD4, CD8 or MHC II and analysed. The data were expressed as the percentage of CD3+ cells in CD11a+ leucocytes, the percentage of CD4+ and CD8+ cell subsets in CD3+ cells, and the percentage of IA-IA+/CD11a+ cells. The data presented are the averages of three experiments.

ation than those from Tg-BO mice, to both superantigens ($P < 0.01$ and $P < 0.001$).

The epidermis of skin lesions are infiltrated by T cells and has accumulation of MHC II+ cells

Our previous study revealed that there were large numbers of mononuclear cells infiltrating in both epidermis and dermis [11]. In the present experiment, we determined the phenotype of cells involved in the inflammation and/or immune response in the skin using immunofluorescence microscopy. In the epidermis, we detected T cells (CD3+, CD4+, and CD8+) (Fig. 6a,b) and found a progressive increase of these

cells as the disease progresses. The number of CD3+ T cells in the epidermis of Tg-LL mice was significantly higher than that found in the skin biopsies from non-Tg mice, in Tg-EL mice, or in the nonlesional skin of diseased mice (Tg-NL) (all with $P < 0.001$; Fig. 6b). While CD4+ and CD8+ cells were not observed in the epidermis of neither Non-Tg nor Tg-NL skin, they were detected in the skin of Tg-EL and Tg-LL mice (Fig. 6b). The number of CD8+ cells (1.83 ± 0.52) in the Tg-LL mice was significantly higher than that of Tg-EL mice (0.77 ± 0.8; $P < 0.05$) (Fig. 6b). The average numbers of CD8+ cells in the epidermis of early and late skin lesions were higher relative to CD4+ cells (Fig. 6b). In addition, the number of MHC II+ cells, most probably Langerhans' cells,
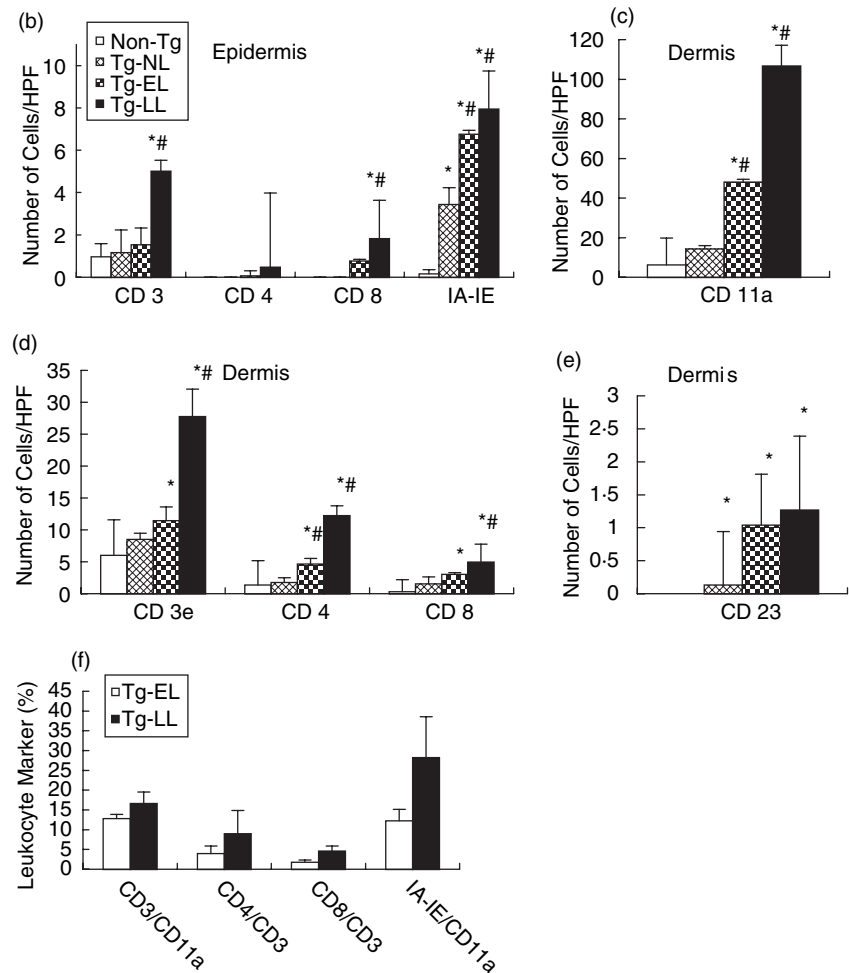
Fig. 6. *Continued.*

significantly increased ($3·44 \pm 0·79$) in the epidermis of Tg-BO skin compared to non-Tg skin ($0·16 \pm 0·2$) ($P < 0·001$). As the disease reached Tg-EL and Tg-LL stages, the numbers elevated to $6·75 \pm 0·19$ and $7·95 \pm 1·8$, respectively, which were significantly higher than those of Tg-BO and non-Tg mice ($P < 0·001$). However, there was no marked difference between Tg-EL and Tg-LL (Fig. 6b).

Progressive increase of CD11a+ leucocytes, T cells and macrophages in the dermis as the disease progresses

In all type cells (CD11a+ leucocytes, CD3+ T cells, CD4+ T cells, CD8+ T cells, CD23+ macrophages) examined, we observed progressive increase in dermal cell numbers as the disease progresses, in comparison to that noted in non-Tg mice (Fig. 6c–e). The numbers of inflammatory cells identified by all five markers (CD11a, CD3, CD4, CD8 and CD23) were significantly higher in the dermis of diseased skin (Tg-EL and Tg-LL) relative to the skin of non-Tg mice ($P < 0·05$ to $P < 0·001$) (Fig. 6c–e). The numbers of dermal CD4+ cells in each of four study groups were more than that of CD8+ cells and these findings were the opposite of the results

obtained in the epidermis. Significantly higher numbers of CD4+ cells than CD8+ cells were determined ($P < 0·0001$). DX5 Abs did not detect the presence of NK cells in the skin samples tested.

In order to substantiate the immunofluorescence microscopy findings, cells obtained from skin samples were analysed for T cells, major T cell subsets, and MHC II by FACS. As illustrated in Fig. 6f, the CD3+ T cells, CD4+ T cells and CD8+ T cells increased in the Tg-LL stage, relative to Tg-EL stage, and these trends were consistent with data demonstrated by fluorescence microscopy (Fig. 6a–e). MHC II+ cells also showed a similar increase (Fig. 6f) as demonstrated in Fig. 6b. Due to the very small numbers of leucocyte present in the skin of non-Tg mice and Tg-BO mice, we were not able to perform FACS analyses on these mice for comparison.

Discussion

Our study first focused on T cells because of their central role in the adaptive immune response. We found that as the disease progressed, T cell numbers were reduced from the

secondary lymphoid organs (spleen and LNs) and increased in the affected skin. The reduction in the percentage and total numbers of T cells from the secondary lymphoid organs could be due to: (1). Increases in non-T cells in the lymphoid organs; (2). T cell death in the lymphoid organs; or (3). Migration of T cells from secondary lymphoid organs into the skin. Although the reduction of T cell percentage in lymphoid organs (Fig. 1a) could be due to the corresponding increase in dendritic cells, macrophages, and NK cells (Figs 2–4), one could not satisfactorily explain the reduction of total number of T cells in lymphoid organs solely by the increase of these non-T cells (Fig. 1Ab). Furthermore, one cannot attribute the decrease of T cells entirely on cell death, because these T cells exhibited the ability to proliferate spontaneously and to proliferate in an enhanced manner by stimulants as the disease progresses, comparing to that of non-Tg mice (Fig. 5). In addition, the percentage of CD4+ and CD8+ T cells expressing activation markers (CD44 and CD69) and costimulatory molecules (ICOS and PD-1), showed a progressive increase trend in the Tg mice as the disease progresses, relative to non-Tg mice (Fig. 1e–h; Fig. 1k–n). Moreover, T cell numbers increased in the skin epidermis and dermis as the disease progressed (Fig. 6). Together, the reduction of T cells from lymphoid organs while increasing their activation status and the increase of T cells in the skin, as the disease progresses suggesting that T cells might have migrated from the secondary lymphoid organs into the skin. The other evidence supporting the migration of T cells to the skin is provided by our previously reported findings that adhesion molecules (ICAM-1, VCAM-1, E-selectin and P-selectin) in the dermal endothelia of diseased skin were highly up-regulated [19]. In addition, the finding that the number of P-Selectin glycoprotein ligand-1+ skin infiltrating cells was substantially increased in the dermis of diseased skin also supports this notion of inflammatory cell migration [19].

One of the most interesting and potentially important findings regarding the characteristics of lymphoid organ CD11c+ dendritic cells is that the highest average percent and the total combined number of CD11c+ dendritic cells, as well as the highest average percent of CD86+, B7 h+, and B7-DC+ dendritic cells, were observed in the Tg-BO mice (Fig. 2). Since one of the major functions of APCs, such as dendritic cells, is to capture the antigen, migrate to the lymphoid organs and present the processed antigen to the T cells, we speculate that the increase in CD11c+ cells in the lymphoid organs might reflect a net movement from the periphery, for the purpose of antigen presentation. Since antigen presentation precedes T cell activation and effector functions that ultimately lead to clinically observable phenotype, these increases of dendritic cell numbers and their surface costimulatory molecules in the Tg-BO mice are consistent with this well-documented immunological sequence of events. This interpretation is further supported by the results from the skin draining LN cell proliferation

assays. The cells in the LNs proliferate spontaneously and the proliferation is enhanced with the addition of superantigens and other stimulants. The spontaneous proliferation of LN cells indicated that these cells are likely in higher state of activation, perhaps due to continual stimulation provided by the influx of antigen- or allergen-bearing APCs. Although we have not identified the antigen/allergen involved in the disease development, given our observation that inflammatory skin lesions occurred predominantly on hairless areas and that the mice do not develop skin lesions until few weeks after birth, we hypothesize that exposure to antigen/allergen is probably needed to initiate the skin inflammatory process in the presence of local IL-4. Further experiments need to clarify this point.

The changes occurred in lymphoid organ monocytes/macrophages observed in our mouse model are somewhat different than that in lymphoid organ dendritic cells. The average percent and the total combined numbers of Mac3+ cells remained relatively unchanged or slightly increased until Tg-LL stage, where a prominent increase occurred (Fig. 3). In the skin, the affected organ, small numbers of CD23+ macrophages were found in the dermis of skin lesions in Tg-EL and Tg-LL mice, and in nonlesional skin of Tg mice, whereas they are not detected in the skin of non-Tg mice (Fig. 6e). We incline to interpret these data to suggest that macrophage subset of APCs may not be essential in the induction of inflammation in our model, but may participate in the maintenance of inflammation. To exclude the possibility of CD23+ cells observed in this study are B cells, we performed CD19 immunofluorescence staining. Result showed that the numbers of CD19+ cells increased as the disease progressed (Tg-EL, 0.32 ± 0.2 and T-LL 0.43 ± 0.2/HPF) relative to the skin of Tg-NL (0.09 ± 0.08/HPF), while they were not detected in non-Tg mice (unpublished data). However, the number of B cells present in the dermis was significant lower than that of CD23+ cells (Tg-EL: 1.04 ± 0.77, Tg-LL: 1.27 ± 1.12, Tg-NL: 0.13 ± 51, $P < 0.05$ compared to B cell counts). Therefore, even though the activated B cells may constitute a small percentage of the CD23+ cells (Fig. 6e), the majority of the CD23+ cells should not be B cells, but macrophage.

The changes of NK cells of the lymphoid organs in our studies showed a generally increasing trend as the disease progresses, with the most pronounced increase occurred in Tg-LL mice (Fig. 4). Relative to LNs, the percent of NK cells in the spleen is higher (Fig. 4). Since we were not able to detect the presence of NK cells in the affected skin, the significance of these increases of NK cells in the secondary lymphoid organs is not clear.

The spontaneous proliferation of cells obtained from LNs of Tg-EL or Tg-LL mice was significantly higher than that of cells from non-Tg mice (Fig. 5). Considering the fact that T cells among CD11a+ leucocytes in the LNs of Tg-LL mice is about 30% of that present in the LNs of non-Tg mice (Fig. 1a–h) and that same numbers of total LNs cells were

used in the cell proliferation assay, the difference in spontaneous proliferation between Tg-LL and non-Tg mice would be considerably higher than that shown in Fig. 5, if equal numbers of T cells were used for the proliferation assays. Thus the activation and expansion undergone by these T cells were actually more vigorous than shown (Fig. 5). Our data on enhanced proliferation of the cells obtained from LNs of the diseased IL-4-Tg mice in response to superantigen stimulation is consistent with earlier findings in children and adult patients with AD in several previous studies showing significantly increased responses of peripheral blood mononuclear cells to SEA and SEB [20–22].

In our mouse model, the percentage of T cells (both CD4+ and CD8+) that are CD44+ and CD69+ increased as the disease progressed. However, the percent of CD3+ T cells among all CD11a+ leucocytes and the percent of CD28+ T cell subsets decreased precipitously, in the lymphoid organs (Fig. 1). CD44 is a cell adhesion molecule present on the surface of activated T cells and is the major cell surface receptor for the glycosaminoglycan, hyaluronan (HA), which is an integral component of extracellular matrix [23]. CD44 is now known to be up-regulated in response to antigenic stimuli, and can mediate leucocyte rolling on endothelial cells and tissue matrix, and lymphocyte activation and homing. In addition, it may participate in the effector stage of immune response, and have broader functions in cellular signalling cascades [23–27]. A portion of these CD4+/CD44+ T cell subset may be memory T cells, which express high levels of CD44 and low levels of CD25 [28]. CD69, also known as activation inducer molecule, is an early cell surface antigen expressed by T cells following activation [29,30]. Once expressed, CD69 acts as a costimulatory molecule for T cell activation and proliferation and has been implicated in the involvement of inflammatory diseases such as rheumatoid arthritis, late inflammatory liver diseases, and asthma [29,30]. Together, increases in CD44+ and CD69+ T in the secondary lymphoid organs of the Tg mice as the disease progresses support the notion that there is constant replenishment of activated memory T cell subset in these lymphoid organs that most likely replace cells migrating into the affected skin.

It is now well understood that an optimal T cell activation requires a primary T cell receptor (TCR) signalling by the MHC-antigenic peptide presented through the APCs and a second antigen-independent signal provided by the costimulatory molecules present on both T cells and APCs [18]. Recently, in addition to the classic costimulatory molecules CD28/CTLA-4 on T cells and the B7-1/B7-2 on APCs, additional members have been identified on T cells and APCs [18,31–33]. ICOS, expressed on activated T cells, has a potent costimulatory activity, and is critical for CD40-mediated Ab class switching that leads to humoral immune response [18,31,33]. The expression of ICOS seems to have a relative, but not absolute, dependence on signals from TCR and CD28, since human CD8+ T cells can express

ICOS in the absence of CD28 [31,34]. The ligand for ICOS, ICOSL, or B7 h, a member of Ig superfamily, is constitutively expressed on un-stimulated APCs, including B cells, macrophages, and dendritic cells, but its expression is enhanced by TNF-α [31,35,36]. Unlike CD28 costimulation, which appears to have a nonredundant role in the initial activation of IL-2 production critical for immune response initiation, the subsequent ICOS costimulation is more important for augmenting IL-10 production and enhancing effector functions [31]. Furthermore, it is now determined that Th2 cytokine production has a greater dependence on ICOS costimulation than the Th1 cytokine production and that antagonism of ICOS costimulation seems to be more effective during the later part of immune response [31,37]. In the lymphoid organs of our IL-4-Tg mice with skin disease, the percent of ICOS+ T cell subsets (both CD4+ and CD8+) increased, but this increase was observed primarily in the later part of the inflammation, i.e. in the Tg-LL stage (Fig. 1k,l). These findings seem to support the notions that the T cell activation seems to favour a Th2-type immune response and that the ICOS may play a more significant role during the later part of immune response in our model.

PD-1, another member of the Ig superfamily and a type I transmembrane receptor, was originally identified in a T cell line undergoing activation-induced cell death [38]. Resting T or B cells do not express PD-1, but activation through antigen or mitogen receptor can result in surface PD-1 induction [31]. Subsequently, two ligands for PD-1, PD-L1 and PD-L2, have been identified. Resting B cells, monocytes, or dendritic cells do not express either PD-L1 or PD-L2, unless they are activated by antigen receptor, LPS, or IFN-γ [31]. The interaction of PD-1 with either ligand (PD-L1 or PD-L2) can result in similar immune outcomes, suggesting that these two ligands have overlapping functions *in vivo* [31]. Engagement of PD-1 with its ligands has been reported to have strong inhibitory effects on T cell proliferation and cytokine production [31,32,39]. However, two separate groups of investigators have concluded that PD-L1/B7 h and PD-L2/B7-DC can be positive costimulatory molecules for T cell proliferation and cytokine production, raising the possibility that there may be additional, yet undiscovered, T cell receptors for PD-L1 and PD-L2 [31,40,41]. Whether the expressions of PD-1 and PD–L2 and their interaction in our IL-4-Tg mice lymphoid organs actually result in negative or positive immune response is not clear. However, what is clear is that even if their interactions resulted in negative regulatory immune response, it was not sufficient to overcome the positive regulatory immune response by the interaction of ICOS and ICOSL, as indicated by the results of T cell proliferation assays (Fig. 5).

In the affected skin, numerous CD11a+ leucocytes were found infiltrating the dermis of IL-4-Tg with early and late disease, including CD3+ T cells (CD4+ and CD8+) (Fig. 6a,b), CD23+ macrophages (Fig. 6e). Furthermore,

CD4+ T cells dominated the dermal T cell infiltrate, which is consistent with the findings in human AD patients [42]. Previously, we have demonstrated a significant infiltration of mast cells into the dermis of Tg mice with early or late disease along with some eosinophils in the dermis of Tg mice with late disease [11]. The progressive increase of MHC II+ cells in the epidermis (Fig. 6b) indicated that there was accumulation of these cells, which was consistent with the study by Elbe-burger *et al.* [16]. However, we currently do not know if there is an impairment of the emigration of these cells. Therefore, it is possible that these different types of leucocyte infiltrates may, to varying degrees, participate in the pathogenesis of AD. Future studies using knock out mice with single cell type target mutation may be helpful in delineating the degrees of involvement of each of these inflammatory cell types [43].

Taken together, we observed that as the disease progresses, the T cells from IL-4-Tg mice showed a spontaneous proliferation and a progressively enhanced proliferative response to stimulants; the percent of T cells expressing certain activation molecules and costimulatory molecules were progressively increased; the percent and the total numbers of T cell were reduced in an incremental manner in the secondary lymphoid organs while the number of T cells infiltrating the skin increased in an incremental fashion; the total number of dendritic antigen presenting cells, macrophages, and NK cells showed gradual increases in the lymphoid organs. Collectively, our results suggest that there is a continued and progressive migration of activated inflammatory cells from the secondary lymphoid organs into the skin where they participate in immune responses resulting in the pathology associated with inflammation.

Acknowledgement

References

1 Cooper KD. Atopic dermatitis. recent trends in pathogenesis and therapy. J Invest Dermatol 1994; **102**:128–37.

2 Leung DY, Bieber T. Atopic dermatitis. Lancet 2003; **361**:151–60.

3 Hamid Q, Boguniewicz M, Leung DY. Differential in situ cytokine gene expression in acute versus chronic atopic dermatitis. J Clin Invest 1994; **94**:870–6.

4 Hamid Q, Naseer T, Minshall EM, Song YL, Boguniewicz M, Leung DY. In vivo expression of IL-12 and IL-13 in atopic dermatitis. J Allergy Clin Immunol 1996; **98**:225–31.

5 Braathen LR, Forre O, Natvig JB, Eeg-Larsen T. Predominance of T lymphocytes in the dermal infiltrate of atopic dermatitis. Br J Dermatol 1979; **100**:511–9.

6 Leung DY, Bhan AK, Schneeberger EE, Geha RS. Characterization of the mononuclear cell infiltrate in atopic dermatitis using monoclonal antibodies. J Allergy Clin Immunol 1983; **71**:47–56.

7 Zachary CB, Allen MH, MacDonald DM. In situ quantification of T-lymphocyte subsets and Langerhans cells in the inflammatory infiltrate of atopic eczema. Br J Dermatol 1985; **112**:149–56.

8 Lugovic L, Lipozenocic J, Jakic-Razumovic J. Atopic dermatitis: immunophenotyping of inflammatory cells in skin lesions. Int J Dermato 2001; **1**:489–94.

9 Woodward AL, Spergel JM, Alenius H. et al. An obligate role for T-cell receptor alphabeta+ T cells but not T-cell receptor gammadelta+ T cells, B cells, or CD40/CD40L interactions in a mouse model of atopic dermatitis. J Allergy Clin Immunol 2001; **107**:359–66.

10 Mihm MC Jr, Soter NA, Dvorak HF, Austen KF. The structure of normal skin and the morphology of atopic eczema. J Invest Dermatol 1976; **67**:305–12.

11 Chan LS, Robinson N, Xu L. Expression of interleukin-4 in the epidermis of transgenic mice results in a pruritic inflammatory skin disease: an experimental animal model to study atopic dermatitis. J Invest Dermatol 2001; **117**:977–83.

12 Hanifin JM, Rajka G. Diagnostic features of atopic dermatitis. Acta Derm Venereol 1980; **92**:44–7.

13 Lee F, Yokota T, Otsuka T. et al. Isolation and characterization of a mouse interleukin cDNA clone that expresses B-cell stimulatory factor 1 activities and T-cell-and mast-cell-stimulating activities. Proc Natl Acad Sci USA 1986; **A83**:2061–5.

14 Chen L, Martinez O, Overbergh L, Mathieu C, Prabhakar BS, Chan LS. Early upregulation of Th2 cytokines and late surge of Th1 cytokines in an atopic dermatitis model. Clin Exp Immunol 2004; **138**:375–87.

15 Lever WF, Schaumberg-Lever G. Histopathology of the Skin, 6th Edn. Philadelphia: J.B. Lippincott Co, 1983:99.

16 Elbe-Burger A, Egyed A, Olt S, Klubal R, Mann U, Rappersberger K, Rot A, Stingl G. Overexpression of IL-4 alters the homeostasis in the skin. J Invest Dermatol 2002; **118**:767–78.

17 Braathen LR. T-cell subsets in patients with mild and severe atopic dermatitis. Acta Derm Venereol (Suppl)(Stockh) 1985; **114**:133–6.

18 Chambers CA. The expanding world of co-stimulation: the two-signal model revisited. Trends Immunol 2001; **22**:217–23.

19 Venkataramani P, Grzeszkiewicz T, Lin SX, Prabhakar BS, Chan LS. An animal model of atopic dermatitis: lesional skin immunophenotyping delineates a CD4+ T cell-predominated inflammatory infiltrate associated with up-regulation of adhesion molecule. J Invest Dermatol 2003; **121**:Abstract no. 44.

20 Campbell DE, Kemp AS. Proliferation and production of interferon-gamma (IFN-gamma) and IL-4 in response to Staphylococcus aureus and staphylococcal superantigen in childhood atopic dermatitis. Clin Exp Immunol 1997; **107**:392–7.

21 Davison S, Allen M, Vaughan R, Barker J. Staphylococcal toxin-induced T cell proliferation in atopic eczema correlates with increased use of superantigen-reactive Vbeta-chains in cutaneous lymphocyte-associated antigen (CLA)-positive lymphocytes. Clin Exp Immunol 2000; **121**:181–6.

22 Yudate T, Yamada H, Tezuka T. Role of staphylococcal enterotoxins in pathogenesis of atopic dermatitis. growth and expression of T cell receptor V beta of peripheral blood mononuclear cells stimulated by enterotoxins A and B. J Dermatol Sci 1996; **13**:63–70.

23 Goodison S, Urquidi V, Tarin D. CD44 cell adhesion molecules. Mol Pathol 1999; **52**:189–96.

24 Haynes BF, Telen MJ, Hale LP, Denning SM. CD44-a molecule involved in leukocyte adherence and T-cell activation. Immunol Today 1989; **10**:423–8.

25 Lesley J, Hyman R, Kincade PW. CD44 and its interaction with extracellular matrix. Adv Immunol 1993; **54**:271–335.

26 Pure E, Cuff CA. A crucial role for CD44 in inflammation. Trends Mol Med 2001; **7**:213–21.

27 Ponta H, Sherman L, Herrlich PA. CD44: from adhesion molecule to signaling regulators. Nat Rev Mol Cell Biol 2003; **4**:33–45.

28 Dutton RW, Bradley LM, Swain SL. T cell memory. Annu Rev Immunol 1998; **16**:201–23.

29 Ziegler SF, Ramsdell F, Alderson MR. The activation antigen CD69. Stem Cells 1994; **12**:456–65.

30 Marzio R, Mauel J, Betz-Corradin S. CD69 and the regulation of the immune function. Immunopharmacol Immunotoxicol 1999; **21**:565–82.

31 Carreno BM, Collins M. The B7 family of ligands and its receptors. new pathways for costimulation and inhibition of immune responses. Annu Rev Immunol 2002; **20**:29–53.

32 Latchman Y, Wood CR, Chernova T. *et al.* PD-L2 is a second ligand for PD-1 and inhibits T cell activation. Nature Immunol 2001; **2**:261–8.

33 McAdam AJ, Greenwald RJ, Levin MA, Chernova T, Malenkovich N, Ling V, Freeman GJ, Sharpe AH. ICOS is critical for CD40-mediated antibody class switching. Nature 2001; **409**:102–5.

34 Hutloff A, Dittrich AM, Beier KC, Eljaschewitsch B, Kraft R, Anagnostopoulos I, Korczek RA. ICOS is an inducible T-cell co-stimulator structurally and functionally related to CD28. Nature 1999; **397**:263–6.

35 Swallow MM, Wallin JJ, Sha WC. B7h, a novel costimulatory homolog of B7.1 and B7.2, is induced by TNGalpha. Immunity 1999; **11**:423–32.

36 Yoshinaga SK, Whoriskey JS, Khare SD. *et al.* T-cell co-stimulation through B7RP-1 and ICOS. Nature 1999; **402**:827–32.

37 Gonzalo JA, Tian J, Delaney T. *et al.* ICOS is critical for T helper cell-mediated lung mucosal inflammatory responses. Nature Immunol 2001; **2**:597–604.

38 Ishida Y, Agata Y, Shibahara K, Honjo T. Induced expression of PD-1, a novel member of the immunoglobulin gene superfamily, upon programmed cell death. EMBO J 1992; **11**:3887–95.

39 Freeman GJ, Long AJ, Iwai Y. *et al.* Engagement of the PD-1 immunoinhibitory receptor by a novel B7 family member leads to negative regulation of lymphocyte activation. J Exp Med 2000; **192**:1027–34.

40 Dong H, Zhu G, Tamada K, Chen L. B7–H1, a third member of the B7 family, co-stimulates T-cell proliferation and interleukin-10 secretion. Nature Med 1999; **5**:1365–9.

41 Tseng SY, Otsuji M, Gorski K. *et al.* B7-DC, a new dendritic cell molecule with potent costimulatory properties for T cells. J Exp Med 2001; **193**:839–46.

42 Reinhold U, Kukel S, Goeden B, Neumann U, Kreysel HW. Functional characterization of skin-infiltrating lymphocytes in atopic dermatitis. Clin Exp Immunol 1991; **86**:444–8.

43 Mak TW, Penninger JM, Ohashi PS. Knockout mice: a paradigm shift in moderm immunology. Nature Rev Immunol 2001; **1**:11–9.